X-582-74-207
PREPRINT

NASA TM X- 70720

POST-FLIGHT DIFFERENTIAL CORRECTION ANALYSIS USING VINTI'S SPHEROIDAL METHOD FOR THE SMALL ASTRONOMY SATELLITE ORBIT

HARVEY WALDEN

APRIL 1974

GSFC

GODDARD SPACE FLIGHT CENTER
GREENBELT, MARYLAND

X-582-74-207
PREPRINT

POST-FLIGHT DIFFERENTIAL CORRECTION ANALYSIS USING VINTI'S SPHEROIDAL METHOD FOR THE SMALL ASTRONOMY SATELLITE ORBIT

Harvey Walden

April 1974

NATIONAL AERONAUTICS AND SPACE ADMINISTRATION
GODDARD SPACE FLIGHT CENTER
Greenbelt, Maryland

POST-FLIGHT DIFFERENTIAL CORRECTION ANALYSIS USING VINTI'S SPHEROIDAL METHOD FOR THE SMALL ASTRONOMY SATELLITE ORBIT

Harvey Walden

ABSTRACT

The results of an intensive analysis of a differential orbit improvement method utilizing observational data for a 550-kilometer altitude, near-circular, near-equatorial satellite orbit are presented. The differential correction has previously been formulated analytically from the equations of motion for an accurate intermediary reference orbit based upon the spheroidal theory of artificial satellite motion about an oblate planet, as developed by Vinti. Observations of the Small Astronomy Satellite (SAS-I) utilized in this study are in the form of direction cosines as measured at two ground interferometer tracking stations near the Equator during the first 22 orbital revolutions (approximately 37 hours) after launch of the spacecraft. Numerical results, in both tabular and graphical form, are displayed for numerous iterated fittings of various observational arcs by differential correction of the orbital elements. Parameters varied in these comparative cases include the time duration of the observational data block, the number of pairs of direction cosine data and the number of tracking station passes included in the solution, the distribution of such passes between the two available tracking stations, and the acceptance criterion for the observational

residuals in the least squares fitting procedure. For converged differentially corrected solutions, the standard deviations of fit, the proportional number of accepted observational residuals, and the converged values of the orbital elements are compared. It is found that three observational pairs of direction cosine data, the minimum number possible for a uniquely determined solution in theory, are sufficient to promote convergence to an accurate solution, if properly selected. Also, the minimum observational data block required to produce an accurate converged orbital solution, given the poor longitudinal distribution of tracking stations available, is found to consist of three station passes. Observations from either of the two tracking stations used independently produce essentially equivalent converged solutions as one another and as the combined data solution using observations from both stations. Finally, the nearly singular values of the orbital elements for SAS-I present no difficulties in convergence for the differential correction method.

CONTENTS

	Page
Abstract	iii
INTRODUCTION AND OBJECTIVES	1
SAS MISSION DESCRIPTION	5
BACKGROUND DATA FOR STUDY	9
PRESENTATION OF RESULTS FOR REFERENCE CASES	15
PRESENTATION OF RESULTS FOR COMPARATIVE CASES	31
SUMMARY AND CONCLUSIONS	46
ACKNOWLEDGMENTS	49
REFERENCES	50

ILLUSTRATIONS

Figure		Page
1	Convergence of the Semi-Major Axis Through Iterated Least Squares Fittings of the Differential Solution to SAS Observational Data	21
2	Convergence of the Orbital Eccentricity Through Iterated Least Squares Fittings of the Differential Solution to SAS Observational Data	22
3	Convergence of the Orbital Inclination Through Iterated Least Squares Fittings of the Differential Solution to SAS Observational Data	23
4	Convergence of the Time of Perigee Passage Through Iterated Least Squares Fittings of the Differential Solution to SAS Observational Data	24
5	Convergence of the Argument of Perigee Through Iterated Least Squares Fittings of the Differential Solution to SAS Observational Data	25
6	Convergence of the Right Ascension of the Ascending Node Through Iterated Least Squares Fittings of the Differential Solution to SAS Observational Data	26
7	Standard Deviations of Fit and the Number of Observational Residuals Accepted at Each Iteration of the Fitting Process for the Combined Data Solution	27
8	Standard Deviations of Fit and the Number of Observational Residuals Accepted at Each Iteration of the Fitting Process for the Quito Data Solution	28
9	Standard Deviations of Fit and the Number of Observational Residuals Accepted at Each Iteration of the Fitting Process for the Kourou Data Solution	29

TABLES

Table		Page
1	Comparison of Pre-Launch Nominal A Priori and Post-Launch "Observed" Mean Orbital Elements for the Small Astronomy Satellite	8
2	Geographic Co-ordinates for Tracking Stations Reporting Observations of the Small Astronomy Satellite.	9
3	Sample Observational Data for the Small Astronomy Satellite During First Two Orbital Revolutions.	11
4	Geophysical Parameter Values Adopted for Earth Model in Post-Flight Studies.	13
5	Initial Conditions for the Orbital Elements and Corresponding Inertial Vectors in Post-Flight Studies	14
6	Iterated Fittings of Observational Arcs by Differential Correction: Reference Cases	16
7	Values at Convergence of Iterated Differential Correction: Reference Cases	18
8	Iterated Fittings of Observational Arcs by Differential Correction: Comparative Cases	32
9	Values at Convergence of Iterated Differential Correction: Comparative Cases	37
10	Iterated Fittings of Observational Arcs by Differential Correction: Further Comparative Cases	39
11	Values at Convergence of Iterated Differential Correction: Further Comparative Cases	44

POST-FLIGHT DIFFERENTIAL CORRECTION ANALYSIS USING VINTI'S SPHEROIDAL METHOD FOR THE SMALL ASTRONOMY SATELLITE ORBIT

INTRODUCTION AND OBJECTIVES

Given an initial estimate to a particular satellite orbit in the form of approximate values for the fundamental elements, the method of orbit improvement known as differential correction provides a means of determining a set of orbital elements which more accurately represents the orbital motion. The method of differential correction ordinarily requires the availability of a large number of accurate observations of the orbiting body extending for a certain duration of time. The preliminary estimated orbit is used to obtain computed values for the observational parameters, based upon the tentative orbital elements, at the corresponding observational times. If the elements of the orbit were perfectly accurate, then differences between the computed observational parameters and the actual observed data would not exist; however, in practice, such deviations, known as observational residuals, are almost always non-zero. The residuals result from perturbative influences on the motion not reflected in the preliminary estimation of the orbit. The magnitudes of the residuals are often increased by errors associated with the observations. If the residuals are sufficiently small so that they can be attributed to random errors in the observations, then the orbit obtained at that point in the procedure of orbit correction is considered satisfactory and is referred to as a definitive orbit. The definitive orbit is the end result of the process of differential orbit correction. Such an orbit must, in theory, be based on all the available suitably accurate observations of the orbiting body within the time interval under consideration, and the calculations leading to the determination of the definitive orbit must take into account the exact perturbative effects on the motion. Of course, in practice,

additional observational data for improvement of the orbit often extend ad infinitum and the perturbations cannot be modeled exactly, so that the concept of a definitive orbit and the termination of a differential correction process must be interpreted in a relative sense.

The purpose of a differential correction procedure is to use the observational residuals obtained to improve the approximate values of the orbital elements. This paper will present the results of an analysis of applications of an orbit improvement method to the determination of a definitive orbit for an artificial satellite of the Earth. The method of differential correction utilized in these applications is formulated (Reference 1) on a strictly analytical basis using partial differentiation of the equations of motion. The spheroidal theory of artificial satellite motion, as developed by Vinti (References 2, 3, and 4), is adopted as an accurate intermediary reference orbit for a drag-free satellite moving in the gravitational field of an axially symmetrical oblate planet. In the case of artificial satellites of the Earth, this intermediary reference orbit accounts exactly for the effects of all zonal harmonic terms in the series expansion of the geopotential through the third term, and it accounts for the major portion of the fourth zonal harmonic term as well. The spheroidal theory is applicable to all orbits of arbitrary inclination and eccentricity and contains no so-called critical inclination singularity. The differential correction based upon the spheroidal theory is completely general in the sense that it involves functions only of the mathematical theory of orbital satellite motion and hence is applicable to any type of spacecraft observational data. The process of differential correction removes inaccuracies of the initial conditions (i. e., approximate orbital elements) and accounts for the effects of forces not contained in the analytical model. In this case, such neglected forces include aerodynamic drag, electromagnetic influences, solar radiation pressure, and residual gravitational effects. The orbit improvement results from the calculation of a set of so-called mean orbital elements through an iterative least squares fitting

of the first-order Taylor's series expansion of the conditional equations to a block of observational data. Details of this process are presented elsewhere (References 1 and 5); this paper will emphasize experimental applications of the method.

The primary objective of this investigation is to evaluate the differential correction process based upon the Vinti spheroidal reference orbit. Applications of this method are made to a post-flight analysis of the Small Astronomy Satellite orbit in the time period immediately following launch of the spacecraft. The parameters of this orbit are of particular interest because of its near-circular and near-equatorial character. The orbit altitude is sufficiently great at 550 kilometers so as to avoid severe aerodynamic drag perturbations, at least over the restricted time duration of less than two days which is considered in this study. Cases in which the orbital eccentricity or inclination vanish (or nearly so) have occasionally led to mathematical difficulties or even singularities in analytical theories of orbit determination. Although it has already been well established that these problems do not arise in the use of Vinti's spheroidal theory, previous numerical applications of this method (e.g., References 5 and 6) to artificial Earth satellites have largely been confined to medium inclination orbits. It was felt that a further application of the spheroidal theory in the context of a post-flight differential correction analysis for a more recent satellite mission would be of substantial scientific interest in view of the renewed activity in this area of investigation.

In this study, the capabilities of the differential correction process based upon the Vinti spheroidal reference orbit are examined in a limited observational data environment. Specifically, efforts are undertaken to determine the minimum number of observational data pairs required to achieve convergence of the definitive orbit determination process. Minimization experiments are conducted with respect to the following criteria: the number of tracking stations required to be represented in the solution, the total number of observational

data pairs, the number of individual tracking station passes, and the time duration of the block of observational data included in the differential correction solution. Attempts are made to minimize each of these criteria in turn, using the results of previous calculations as controls.

In the analysis that follows, the efficacy of an individual differentially corrected orbit is judged comparatively by the use of several calculated parameters. The speed of a differential correction is measured by the number of iterations required to achieve convergence in the determination of the final orbital elements. The errors in the final orbital elements are related to the level of convergence of the differential fitting of observational data. This level of convergence is measured by calculating the standard deviation of fit of the least squares process utilized in differential correction (Reference 5). As a second indicator of the level of convergence of the differential correction, the percentage of the total number of observations accepted in the final converged solution may be utilized. However, this is highly correlated to the value used as an acceptance criterion, in terms of standard deviations from the mean for the observational residuals at each iteration of the differential correction. Usually, some pre-selected acceptance tolerance is chosen as a criterion prior to the initiation of differential correction, often one or two sigmas (standard deviations from the mean of the observational residuals). Finally, the converged values for the set of orbital elements for each differential correction may be compared and utilized as a gauge of the quality of the definitive orbit obtained. At this stage, it is important to recall, as stated earlier, that the concept of a definitive orbit must be viewed in a relative sense.

SAS MISSION DESCRIPTION

Application of the differential correction method was made to observations of the Small Astronomy Satellite (abbreviated SAS-I in order to indicate the first spacecraft mission in a project series; international designation 1970 107-A; also known as Explorer 42 and as Uhuru I). This spacecraft was launched from the San Marco platform located in the Indian Ocean off the coast of Kenya, Africa via a four-stage Scout vehicle on December 12, 1970 at $10^h53^m50^s$ Universal Time (U. T.). Injection of the SAS-I spacecraft into a nearly nominal 550-kilometer altitude, circular, near-equatorial orbit occurred approximately 10 minutes following lift-off.

The primary objective (Reference 7) of the SAS-I mission is to detect X-ray sources throughout the celestial sphere and to perform high-sensitivity, high-resolution measurements of these sources to produce an X-ray source catalogue. To accomplish this task, the celestial sphere must be surveyed from above the Earth's atmosphere where X-rays in the energy range of interest (1 to 20 Kev) are absorbed. The equatorial orbit permits the spacecraft to bypass the South Atlantic magnetic anomaly where the radiation belts extend far into the Earth's atmosphere. In addition, the equatorial orbit prevents deterioration of experiment operation and maintains a minimum background count. This background count can adversely affect the data returned from several types of sensors applicable to spacecraft astronomy. Although the nominal prime mission lifetime was specified as six months, the spacecraft has far exceeded original expectations, and, at this writing, is still providing valid and useful astronomical data.

The NASA Space Tracking and Data Acquisition Network (STADAN) station at Quito, Ecuador was the designated (Reference 8) prime tracking facility and gave first priority to the tracking of the SAS-I spacecraft during the early orbital phase following launch and injection. Due to the near-equatorial orbit, no STADAN stations other than Quito were available for interferometer tracking

support. However, the Centre National D'Études Spatiales (CNES) station at Kourou, French Guiana provided supplementary interferometer tracking data during the early orbital phase in its role as designated back-up tracking facility.

A subsidiary objective of the post-flight differential correction analysis presented herein is to evaluate the validity and internal consistency of the interferometer tracking data received from the CNES station at Kourou. These data are in the form of direction cosines as are the so-called Minitrack data received from NASA tracking stations. However, use and application of the French tracking data within NASA have been far less extensive than has been the case with Minitrack data. In fact, the SAS-I mission represented possibly the first occasion in which CNES tracking data were used operationally at NASA for spacecraft early orbit determination. One method of evaluating the validity of the CNES data is to utilize these observations separately in a differential correction of the orbital elements and to compare the resultant values with those obtained from a differential correction based upon Minitrack data only. An associated subsidiary objective of this post-flight analysis is to determine the compatibility of the two types of direction cosine observational data (those obtained from CNES and those from NASA Minitrack) in a single differential correction of orbital elements. This can be accomplished by comparing the results of a differential correction procedure based upon data interspersed from the two sources with the results obtained when either data set is used in isolation. It will be seen that these subsidiary objectives, related to the source of the observational data, were achieved in the initial stages of the post-flight analysis and contribute significantly to the pursuit of the primary objectives of the investigation, as discussed previously.

The SAS-I orbit was determined (in the preliminary estimated sense described earlier) at the Goddard Space Flight Center of NASA approximately 4.5 hours after lift-off, with the author having the responsibility of directing orbital

computations activities (Reference 9). This initial orbit determination was based upon Quito and Kourou interferometer tracking data from the first two orbital revolutions. Table 1 presents a comparison of the pre-launch nominal a priori orbital elements (Reference 10) and the mean orbital elements computed shortly after launch during the initial orbit determination process (Reference 11) utilizing observational data. This latter set of orbital elements is referred to as the "observed" set in contradistinction to the predicted nominal set. In Table 1, the large discrepancy between the nominal and "observed" values for the right ascension of the ascending node is, of course, due to the fact that injection into orbit occurred nearly 5 hours after the nominally scheduled time (based upon a launch delay of this same duration). The nominal value for the right ascension of the ascending node, based upon the actual ("observed") injection time of $11^h 3^m 37.^s 15$ U. T. on December 12, 1970, is 13.931 degrees, considerably closer to the "observed" value for the node. All the "observed" values of the orbital parameters in Table 1 are provided as a point of reference for the initial near-real-time orbit determination procedure as contrasted to the values for these parameters determined in the post-flight differential correction analysis to be described in what follows.

Table 1

Comparison of Pre-Launch Nominal A Priori and Post-Launch "Observed" Mean Orbital Elements for the Small Astronomy Satellite

Orbital Parameter (Units)	Nominal Value	"Observed" Value
Epoch (injection) time (U. T., Dec. 12, 1970)	$6^h 9^m 47^s.15$	$11^h 3^m 37^s.15$
Semi-major axis* (km)	6928.351	6930.095
Eccentricity	0.001507	0.002897
Inclination to Equator (deg)	2.914	3.040
Mean anomaly at epoch (deg)	298.765	288.515
Argument of perigee (deg)	352.376	359.708
Right ascension of ascending node (deg)	300.472	17.521
Anomalistic period (min)	95.654	95.690
Height of perigee * (km)	539.75	531.85
Height of apogee * (km)	560.62	572.01

* Values are based upon an Earth equatorial radius of 6378.166 km.

BACKGROUND DATA FOR STUDY

The direction cosine observational data utilized in this study were taken at one of two tracking stations, located at Quito, Ecuador and Kourou, French Guiana. Table 2 presents the geographic (or geodetic) co-ordinates for these two near-equatorial stations. The fact that the two stations are located within 26 degrees in longitude of one another made the problem of early orbit determination somewhat more difficult than the more commonly encountered case of non-equatorial orbits of medium or high inclination where a better longitudinal distribution of tracking stations is available.

The observational data block included all the data recorded at Quito and Kourou from the time of injection of the SAS-I spacecraft into orbit until the completion of 22 orbital revolutions approximately 37 hours later. This data block includes a total of 33 passes over a tracking station, one each orbital revolution for a total of 22 passes over Quito and an additional 11 passes over Kourou. The Kourou data block includes the first 7 consecutive passes (for purposes of assisting in early orbit determination) and an additional 4 passes of the following 15 passes. During the omitted passes, tracking data were not recorded at the Kourou station for the SAS-I spacecraft. Each recorded pass, both at Quito and Kourou, spanned an interval of 30 seconds in time, with a pair of direction

Table 2

Geographic Co-ordinates for Tracking Stations Reporting Observations of the Small Astronomy Satellite

Tracking Station Name	Longitude* (Deg, Min, Sec)	Latitude* (Deg, Min, Sec)	Altitude* (Meters)
Kourou, French Guiana	307 11 40.92	5 15 3.92	-17.96
Quito, Ecuador	281 25 14.77	-0 37 21.76	3567.07

* Longitude is measured east of Greenwich, latitude is measured north of the Equator (a negative prefix indicates latitude south of the Equator), and altitude is measured above the sea-level geoid (a negative prefix indicates below sea-level altitude).

cosines recorded each 3 seconds, for a total of 11 observations per pass. The totality of observational data was treated in two distinct forms in this study, as "intensive" coverage and as "extensive" coverage. For intensive data coverage, the full 11 observational data pairs per pass were utilized, while for extensive data coverage, only 3 observational data pairs per pass were considered. These 3 data pairs included the first pair recorded, the sixth pair (i. e., the "central" pair) recorded 15 seconds later, and the final pair recorded 30 seconds after the initial pair. The use of extensive data coverage allowed inclusion of observational data over a longer time interval than otherwise, with relatively little loss in informational content (because of the inherent redundancy in observations during a given pass). Also, use of the extensive form permitted the numerical complexities of the mathematical processes (particularly matrix inversions) involved in the differential correction to be kept within reasonable bounds. Table 3 displays a sample portion of the actual observational data utilized in this study reduced to the extensive data coverage form, for the first two orbital revolutions. It is seen that the direction cosines of type "L" progress from negative values through zero to positive values of approximately the same absolute magnitude during the course of a single pass over a station. Meanwhile, the direction cosines of type "M" remain approximately the same magnitude and sign during the pass. The particular range of values assumed by the direction cosines depends upon the elevation angles of the spacecraft relative to the tracking station, but the sign changes are in accordance with the station's geographical location (see Table 2) and the orientation of the inertial co-ordinate system used for measuring the observational data (see footnote to Table 3). Note also from Table 3 that the spacecraft requires about 7.4 minutes to progress eastward from Quito to Kourou, as compared to the full orbital period of 95.7 minutes (see Table 1). Consecutive passes over the same station require an interval of 102.3 minutes, and this value is 6.6 minutes in excess of the orbital period because of the fact that the Earth's rotation is in

Table 3

Sample Observational Data for the Small Astronomy Satellite During First Two Orbital Revolutions

Station Name	Date of Observation (Year, Month, Day)	Time of Observation (Hr, Min, Sec)	Direction Cosine Value	Direct Cosine T
Quito	70 12 12	12 6 27.000	-0.189754 0.281532	L M
Quito	70 12 12	12 6 42.000	-0.010605 0.276226	L M
Quito	70 12 12	12 6 57.000	0.169780 0.263393	L M
Kourou	70 12 12	12 13 50.000	-0.121570 -0.801665	L M
Kourou	70 12 12	12 14 5.000	-0.003034 -0.809946	L M
Kourou	70 12 12	12 14 20.000	0.114538 -0.807523	L M
Quito	70 12 12	13 48 44.000	-0.187567 -0.001350	L M
Quito	70 12 12	13 48 59.000	-0.002084 -0.012258	L M
Quito	70 12 12	13 49 14.000	0.184413 -0.022681	L M
Kourou	70 12 12	13 56 8.000	-0.091389 -0.861224	L M
Kourou	70 12 12	13 56 23.000	0.014016 -0.866005	L M
Kourou	70 12 12	13 56 38.000	0.118426 -0.862064	L M

*The observed direction cosine in the inertial X-direction is denoted "L"; the observed direction cosine in the inertial Y-direction is denoted "M". The inertial co-ordinate system assumes the Earth's polar or rotational as the Z-axis and the Earth's equatorial plane as the X-Y plane, with the axis extending toward the vernal equinox (the first point of Aries). The Y axis extends orthogonally to the east to form a right-handed system, and Earth's center of mass is at the co-ordinate origin.

the same direction as the posigrade (direct) satellite orbit.

During the differential correction studies, a single consistent Earth model was utilized, incorporating the values for geophysical parameters as tabulated in Table 4. Numerical calculations were conducted utilizing the geophysical system of canonical units, as described in the first footnote to Table 4. The set of initial conditions adopted for the orbital elements is given in Table 5. It is seen that the orbital elements are precisely those nominal values displayed in Table 1, with the exception that the right ascension of the ascending node has been updated based upon the actual ("observed" in Table 1) injection time chosen as the epoch time. Also shown in Table 5 is the corresponding set of inertial position co-ordinates and inertial velocity components at epoch time, obtained by the familiar two-body Keplerian transformations.

The weighting factors that were associated with the direction cosine observational data in the differential correction studies were based upon a geometrical criterion. Specifically, the weighting factors associated with the direction cosines L_c and M_c (where the subscripts indicate computed values rather than observed values) are $(1-L_c^2)^{1/2}$ and $(1-M_c^2)^{1/2}$, respectively. This geometrical criterion gives greatest weights (near to the value of unity) when L_c and M_c approach zero, i. e., when arccos L_c and arccos M_c approach 90 degrees. Thus, direct overhead or zenith observations of the spacecraft at the tracking station are given greatest (unit) weight, and horizon observations of the spacecraft are given least (zero) weight. This method of geometrical weighting variation is in accord with the accuracies of the electronic measurement apparatus at the interferometer tracking stations as a function of local elevation angle of the spacecraft position.

Finally, during the present studies, the full differential correction including periodic terms through the second order in the oblateness parameter (Reference 1) was utilized. This is not meant to imply that the shorter first-order treatment for the periodic variables in the differential correction was insufficient for

Table 4

Geophysical Parameter Values Adopted for Earth Model in Post-Flight Studies

Parameter Description (Units)	Usual Symbol	Numerical Value
Earth's equatorial radius, e. r. (km)	r_E	6378.166
Canonical unit of time*, c. u. t. (sec)	t_E	806.81364
Product of Newtonian gravitational constant and Earth's mass, (e. r.^{3}/c. u. t.^{2})	$\mu=GM_E$	1.000
Coefficient of Earth's second gravitational harmonic	J_2	1.08248×10^{-3}
Coefficient of Earth's third gravitational harmonic	J_3	-2.56×10^{-6}
Coefficient of Earth's fourth gravitational harmonic**	J_4	-1.17×10^{-6}
Inverse of Earth's flattening coefficient	1/f	298.25
Earth's rotational rate (rad/sec)	ω_E	7.292115×10^{-5}

*The geophysical system of canonical units adopts the Earth's equatorial radius and the central Earth's mass as the fundamental units of length and mass, respectively. The corresponding canonical unit of time is chosen so that the Newtonian gravitational constant, G, is set equal to unity. The physical significance for this time interval is given by the fact that it represents the time required for a hypothetical Earth satellite moving in the equatorial plane of the Earth at surface altitude to traverse one radian.

** The numerical value given for J_4 is that determined by fitting J_2 and J_3 independently to geodetically obtained values (as shown in the table) in the spheroidal Vinti geopotential. The mathematically constrained value of J_4 is approximately two-thirds of the geodetic value. The mathematically constrained values for higher zonal harmonic coefficients, J_n ($n\geqslant5$), are all negligibly small (Reference 2).

Table 5

Initial Conditions for the Orbital Elements and Corresponding Inertial Vectors in Post-Flight Studies

Orbital Parameter (Units)	Usual Symbol	Initial Value
Epoch (injection) time (U. T., Dec. 12, 1970)	t_0	$11^h 3^m 37^s.15$
Semi-major axis (km)	a	6928.3508
Eccentricity	e	0.0015066
Inclination to Equator (deg)	i	2.914
Mean anomaly at epoch (deg)	M_0	298.765
Argument of perigee (deg)	ω	352.376
Right ascension of ascending node (deg)	Ω	13.931
Inertial position co-ordinates (e. r.)	x_0	0.62105338
	y_0	-0.88875995
	z_0	-0.051520690
Inertial velocity components (e. r./c. u. t.)	$\dot{x}_0$	0.78666682
	$\dot{y}_0$	0.55024491
	$\dot{z}_0$	0.017544538

convergence to be attained; in fact, in past applications, the first-order differential correction has generally been sufficiently accurate to promote convergence in the iterative least squares fitting process. However, in the present application, no attempt was made to determine the efficacy of the first-order version; instead, the more accurate second-order treatment was employed throughout. A final point to be noted is that no atmospheric drag corrections of any type were introduced in the present applications. Methods for correction of atmospheric drag effects are currently under development, but these were not utilized.

PRESENTATION OF RESULTS FOR REFERENCE CASES

In order to provide a comparative basis for the post-flight differential correction analysis, three so-called reference case investigations were undertaken. These reference case studies are also of particular interest in achieving the subsidiary objectives which relate to the source of the observational data. By way of paraphrase, the subsidiary objectives are (1) to evaluate the validity and consistency of CNES tracking data from Kourou, and (2) to determine the compatibility of CNES tracking data and NASA Minitrack data. To these ends, three independent and distinct differential corrections of orbital elements by iterated fittings of observational arcs were performed. Each of the differential corrections began with the same set of initial conditions, as given in Table 5, and utilized the same geophysical parameters for an Earth model, as given in Table 4.

Table 6 displays basic quantitative information about the three reference cases, which are designated by sequential integers for convenience. Case 1 includes 99 observational pairs from both the Quito and Kourou tracking stations, spanning a time interval of almost 36 hours (corresponding to 22 orbital revolutions of SAS-I) and covering a total of 33 station passes, two-thirds of which are associated with Quito. This then is seen to represent the complete set of extensive data coverage, as defined previously, inasmuch as there are 3 observational data pairs per pass. Cases 2 and 3 represent partitions of the first case into separate fittings using the totality of observational data from Quito and from Kourou, respectively. These two differential corrections include 66 observational pairs and 33 pairs, respectively, covering approximately (or exactly) the same time interval of 22 orbital periods and are also of the extensive data coverage form. The extensive form of data coverage was chosen for the reference cases, because, as mentioned previously, this form contains the bulk of the informational content of the intrinsically redundant observations during a given pass and, simultaneously, its use diminishes the mathematical

Table 6

Iterated Fittings of Observational Arcs by Differential Correction: Reference Cases

Case Number	Observational Pairs	Time Span	Number of Passes	Stations Included*	Residual Acceptance Criterion**	Convergence Attained	Iterations Required
1	99	$35^h47^m10^s$	33	22Q-11K	1 σ	yes	7
2	66	$35^h47^m10^s$	22	Q	1 σ	yes	8
3	33	$34^h04^m45^s$	11	K	1 σ	yes	6

*The tracking station at Quito, Ecuador is denoted "Q", and the station at Kourou, French Guiana is denoted "K". Integers preceding the appropriate letter symbol indicate the number of passes included for the respective station.

**The acceptance criterion for the observational residuals during the least squares iterated fitting process utilized in the differential correction is given in terms of "sigmas", or standard deviations from the mean value of the observational residuals at each iteration.

complexities in the differential correction operations (as compared to those engendered by use of the intensive form of data coverage). For all three reference cases, the acceptance criterion for the observational residuals during the iterated differential fitting was chosen to be one sigma. That is to say, if at any iteration in the least squares fitting process, an observational residual is displaced from the mean value of all the observational residuals at that iteration by more than one standard deviation, then it is rejected upon statistical grounds from inclusion in the subsequent fitting process (Reference 5). For normal (Gaussian) distributions, approximately 68.27 percent of the observational residuals should be accepted in the fitting process based upon such a one-sigma criterion; this percentage level will vary with the skewness of the distribution. It is seen from Table 6 that the one-sigma criterion was sufficient to promote convergence in reasonably few iterations for all three reference cases. The final column of Table 6, which lists the number of iterations required to attain convergence in the orbital elements, is the result of a qualitative measure rather than based upon a specific mathematical criterion for convergence. In all the differential correction fittings, a greater number of iterations was performed than was required for convergence. This procedure permitted the determination of the final iteration required for convergence based upon the point at which the standard deviation of fit levels off to its minimum value and the point at which the orbital elements reach essentially converged values that are subsequently affected only by numerical truncation, round-off errors, and other such computational "noise". The iteration which first produces these noteworthy events was invariably unique and easily determined in the absence of a quantitative criterion, as will readily be seen from the figures to be presented in what follows.

Further quantitative information relating to the same three reference cases of differential correction is shown in Table 7. The total number of conditional equations in each fitting is always double the number of observational pairs

Table 7

Values at Convergence of Iterated Differential Correction: Reference Cases

Case Number	Total Conditional Equations	Accepted Residuals	Percentage of Total	Standard Deviation of Fit (all)*	Standard Deviation of Fit (accepted)*	Converged Semi-Major Axis a (km)	Converged Eccentricity e	Converged Inclination i (deg)
1	198	166	83.8	1.017	0.440	6917.362	0.002796	3.0320
2	132	109	82.6	0.974	0.359	6917.365	0.002804	3.0322
3	66	61	92.4	1.207	0.263	6917.384	0.002840	3.0340

*All standard deviations of fit are given in mils (i.e., in dimensionless units of 10^{-3}). The parenthetical word "all" signifies that all of the observational residuals are included in determining the standard deviation of fit; "accepted" indicates that only the observational residuals corresponding to the accepted conditional equations are included in determining the standard deviation of fit.

considered, since a conditional equation results from each observed direction cosine, L_0 and M_0. The remaining columns of Table 7 give values at convergence for various parameters, i. e., values at the iteration indicated in the final column of Table 6 for each case. The number of accepted observational residuals at convergence based upon the acceptance criterion shown in Table 6 (in all three cases, one sigma) is given, as well as the percentage this number represents of the total observational residuals (which is equal to the total conditional equations shown in a preceding column of Table 7). In all three cases, the percentage is well above that to be expected for a normal distribution and a one-sigma criterion, thus indicating a dense grouping of the residuals about their mean or, equivalently, a high level of fitting achieved at convergence. The following two columns show the standard deviations of fit in dimensionless units of mils, one of which includes all of the observational residuals at convergence and the second of which (invariably smaller in value, of course) includes only the accepted observational residuals at convergence. The final three columns of Table 7 give the values at convergence for three significant orbital elements: the semi-major axis a, the eccentricity e, and the inclination i of the orbital plane to the Equator. These converged orbital elements may be compared to the corresponding initial values given in Table 5. It is seen that the differences in values for the converged orbital elements among the three cases are entirely insignificant compared to the differences between initial and final converged values for the orbital elements. This demonstrates that each differential correction leads independently to essentially the same final converged values for the three orbital elements indicated.

Figures 1 through 6 illustrate the determination of a mean set of orbital elements by an iterated least squares fitting of the differential solution to observational data for each of the three reference cases. In each case, the results of ten iterations are shown, although, as indicated in Table 6, this number is in excess of the number of iterations required for convergence of the differential

orrection of orbital elements. Figures 4, 5, and 6 demonstrate that the remaining three orbital elements not included in Table 7, viz., the time τ of passage through perigee (related to the mean anomaly at epoch), the argument of perigee, and the right ascension Ω of the ascending node, also display the characteristic shared by a, e, and i seen previously. That is, the differences among the converged values of the orbital elements τ, ω, and Ω for the three reference cases are negligible in comparison to the differences between initial and final converged values. Hence, each differential correction independently produces essentially equivalent values upon convergence for all six orbital elements. As for the minor differences among the three references cases in the achievement of convergence, it may be noted that the values of each orbital element at each iteration are virtually indistinguishable between the combined data solution (case 1) and the Quito data solution (case 2); the values for each orbital element at each iteration in the Kourou data solution (case 3) differ slightly from the other two reference cases, although the final converged values are insignificantly different for all six elements.

Figures 7 through 9 illustrate the convergence of what is possibly the most significant single parameter in evaluating the efficacy of the differential correction process, viz., the standard deviation of fit. In each figure, the upper curve (or, more properly, sequence of connected line segments) in the main body of the figure represents the standard deviation of fit which includes all of the observational residuals at each iteration, while the lower curve corresponds to the standard deviation of fit which includes only the observational residuals accepted at each iteration of the fitting process. Plotted on the same abscissa at the top of each figure is a curve showing the number of observational residuals (or, equivalently, the number of equations of condition) accepted at each iteration. Figure 7 shows the standard deviations of fit for the combined data solution (reference case 1), which includes a total of 198 observational residuals. Figures 8 and 9 are similar plots for the Quito data

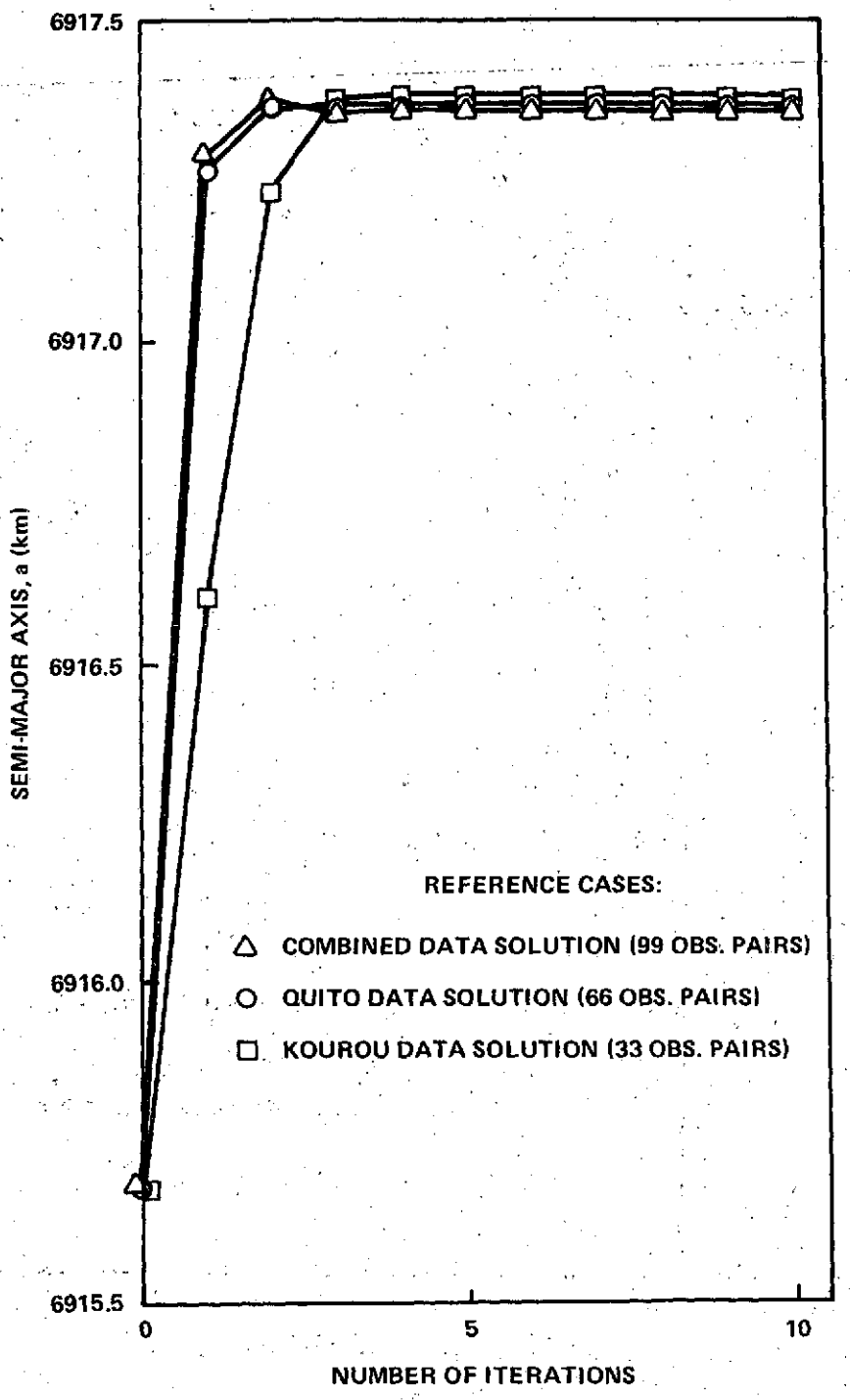

Figure 1. Convergence of the Semi-Major Axis Through Iterated Least Squares Fittings of the Differential Solution to SAS Observational Data

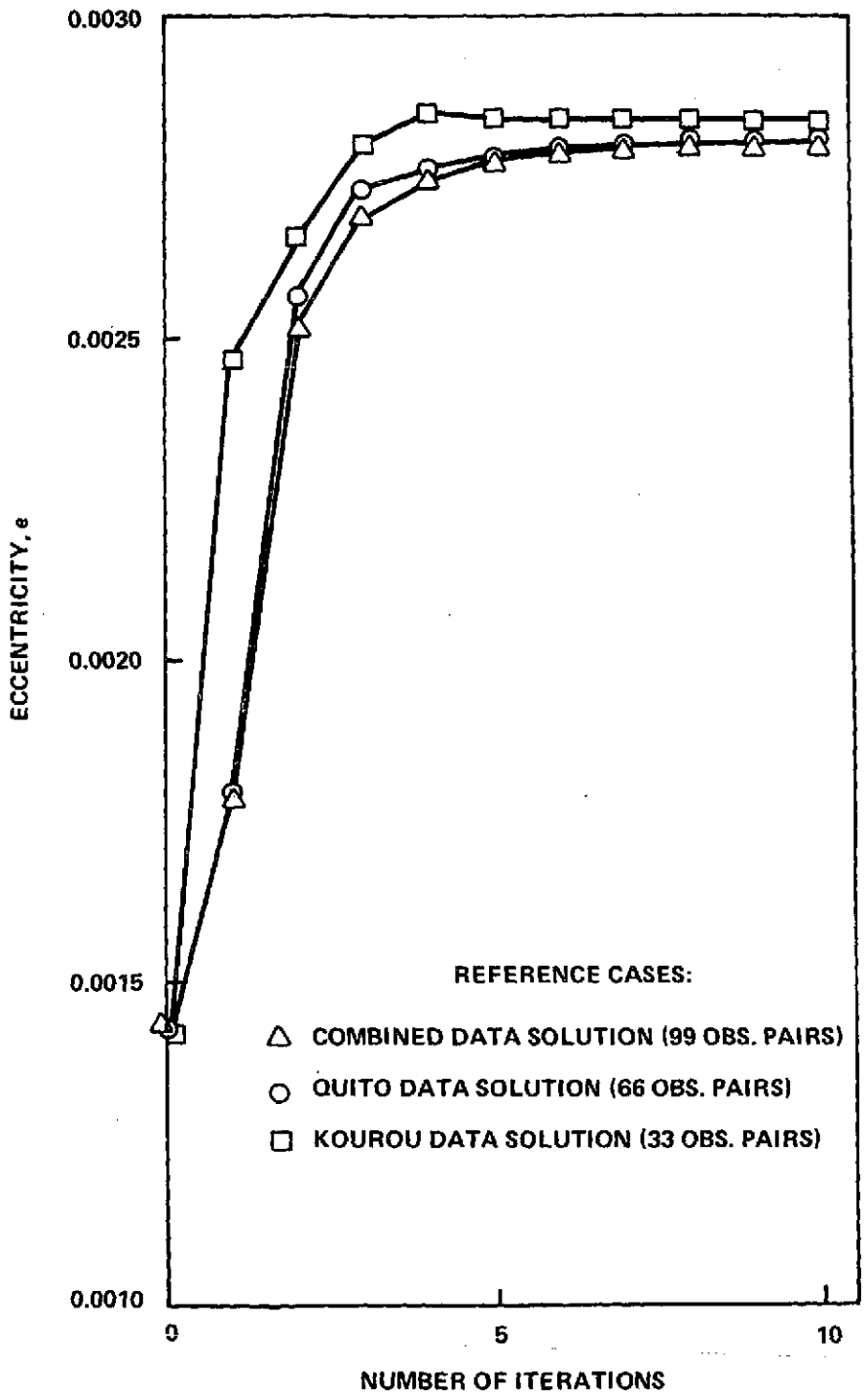

Figure 2. Convergence of the Orbital Eccentricity Through Iterated Least Squares Fittings of the Differential Solution to SAS Observational Data

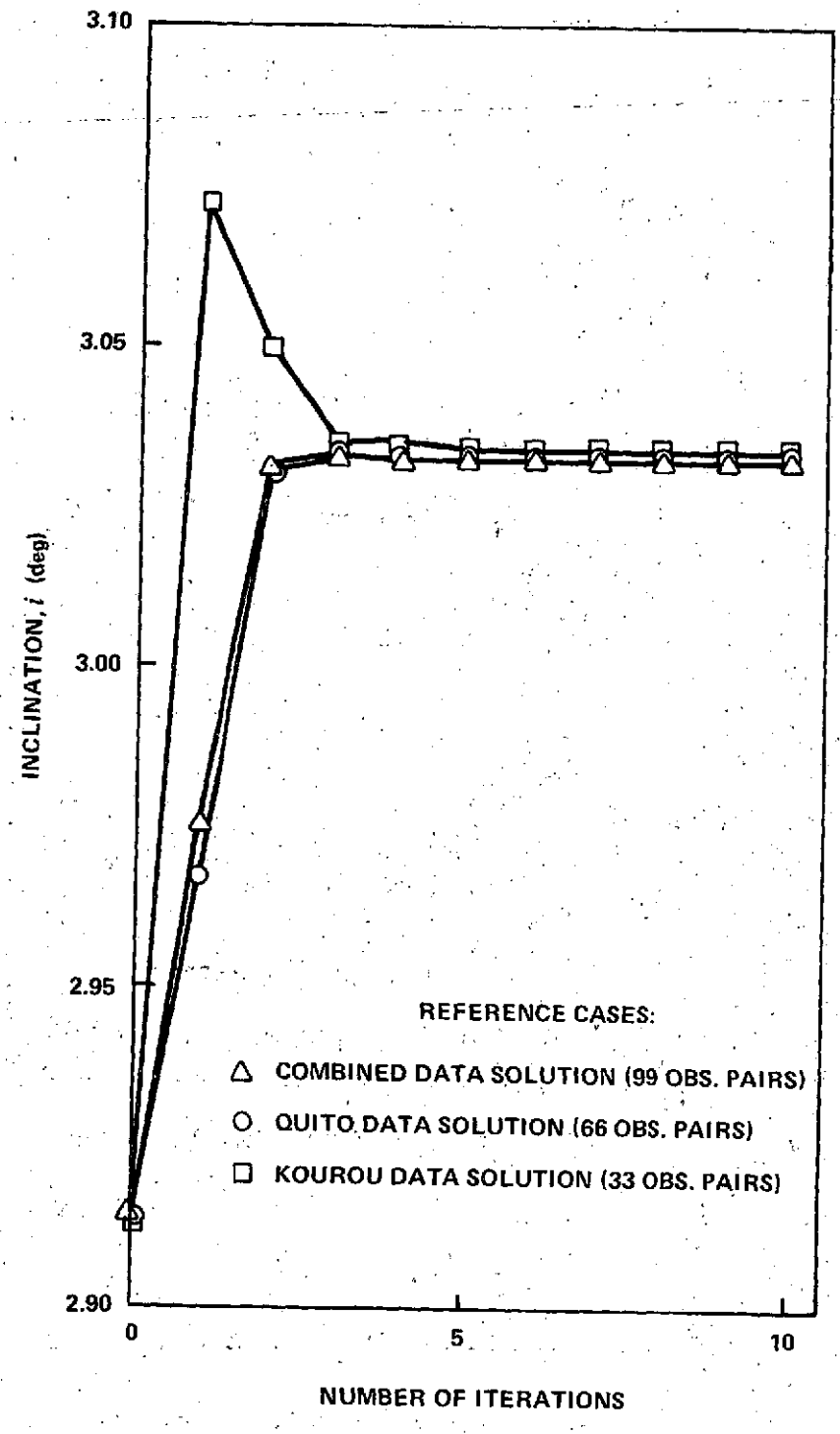

Figure 3. Convergence of the Orbital Inclination Through Iterated Least Squares Fittings of the Differential Solution to SAS Observational Data

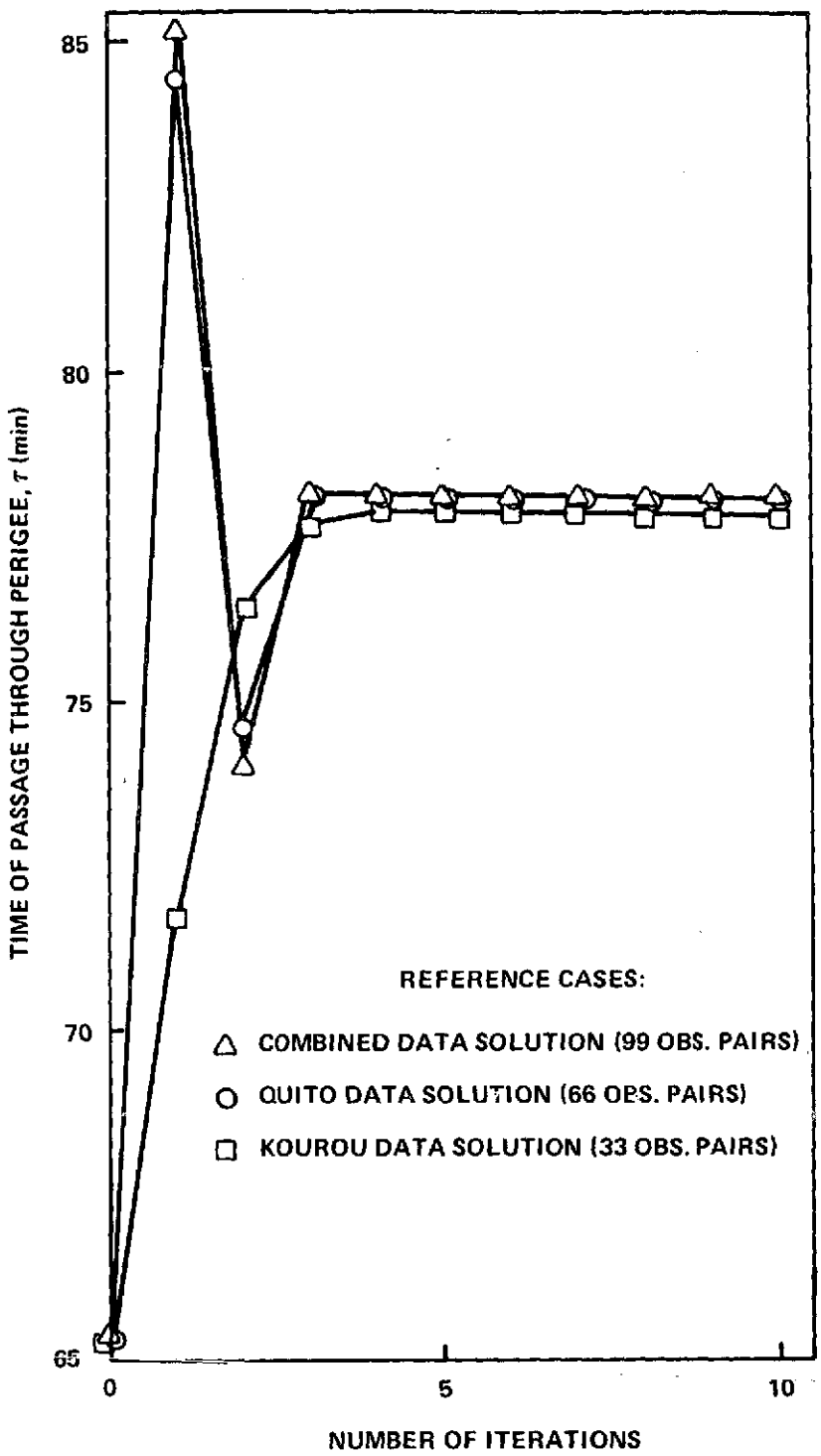

Figure 4. Convergence of the Time of Perigee Passage Through Iterated Least Squares Fittings of the Differential Solution to SAS Observational Data

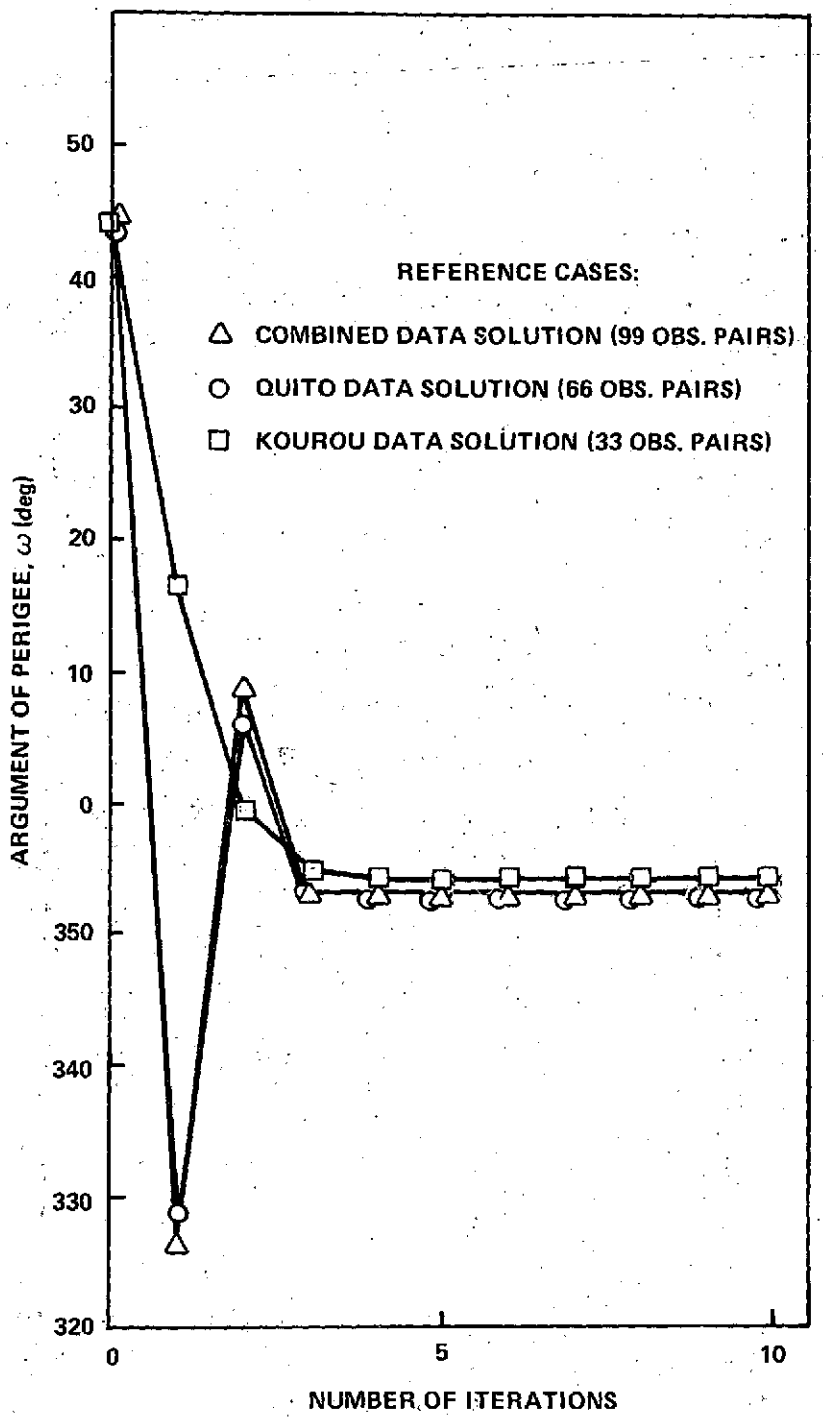

Figure 5. Convergence of the Argument of Perigee Through Iterated Least Squares Fittings of the Differential Solution to SAS Observational Data

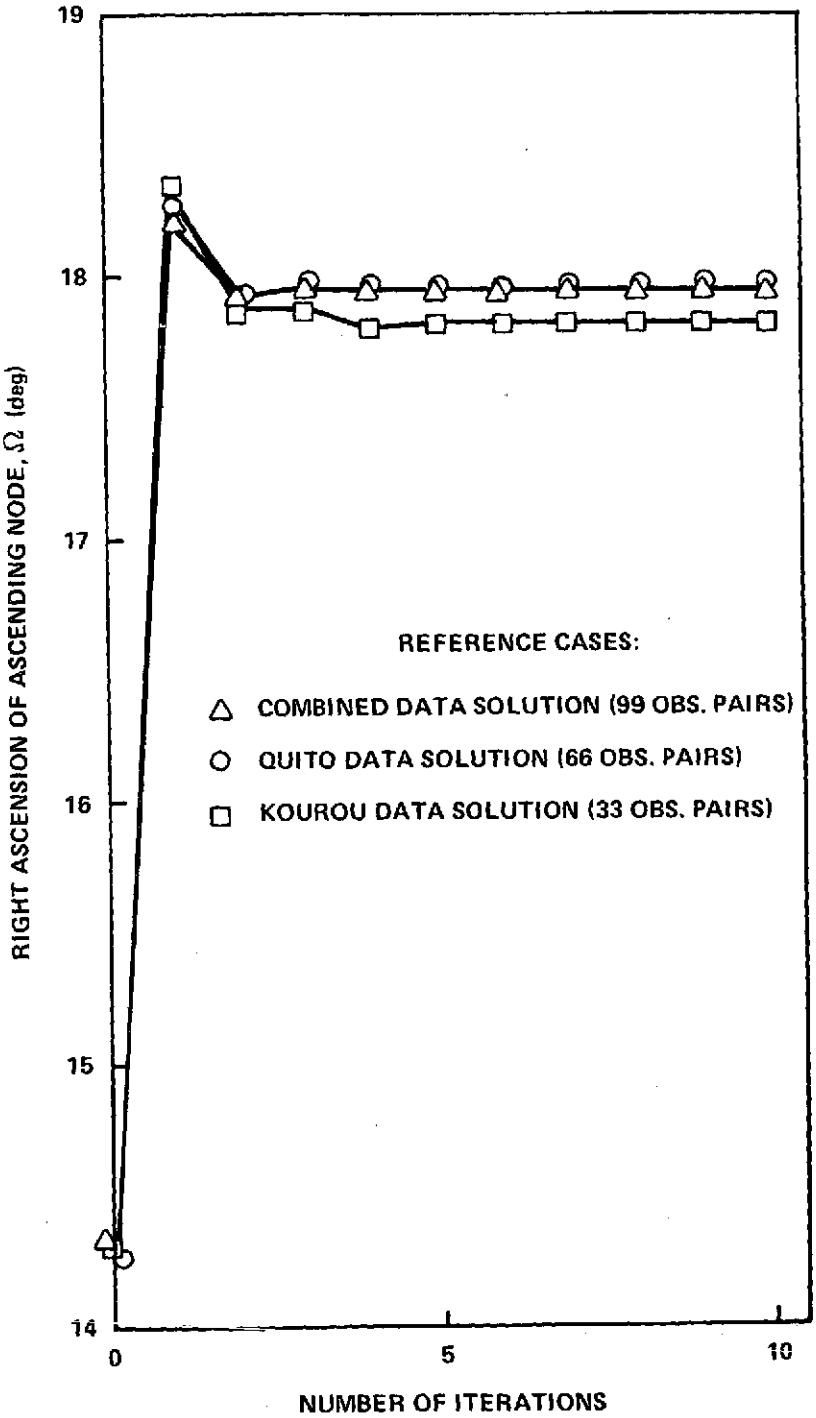

Figure 6. Convergence of the Right Ascension of the Ascending Node Through Iterated Least Squares Fittings of the Differential Solution to SAS Observational Data

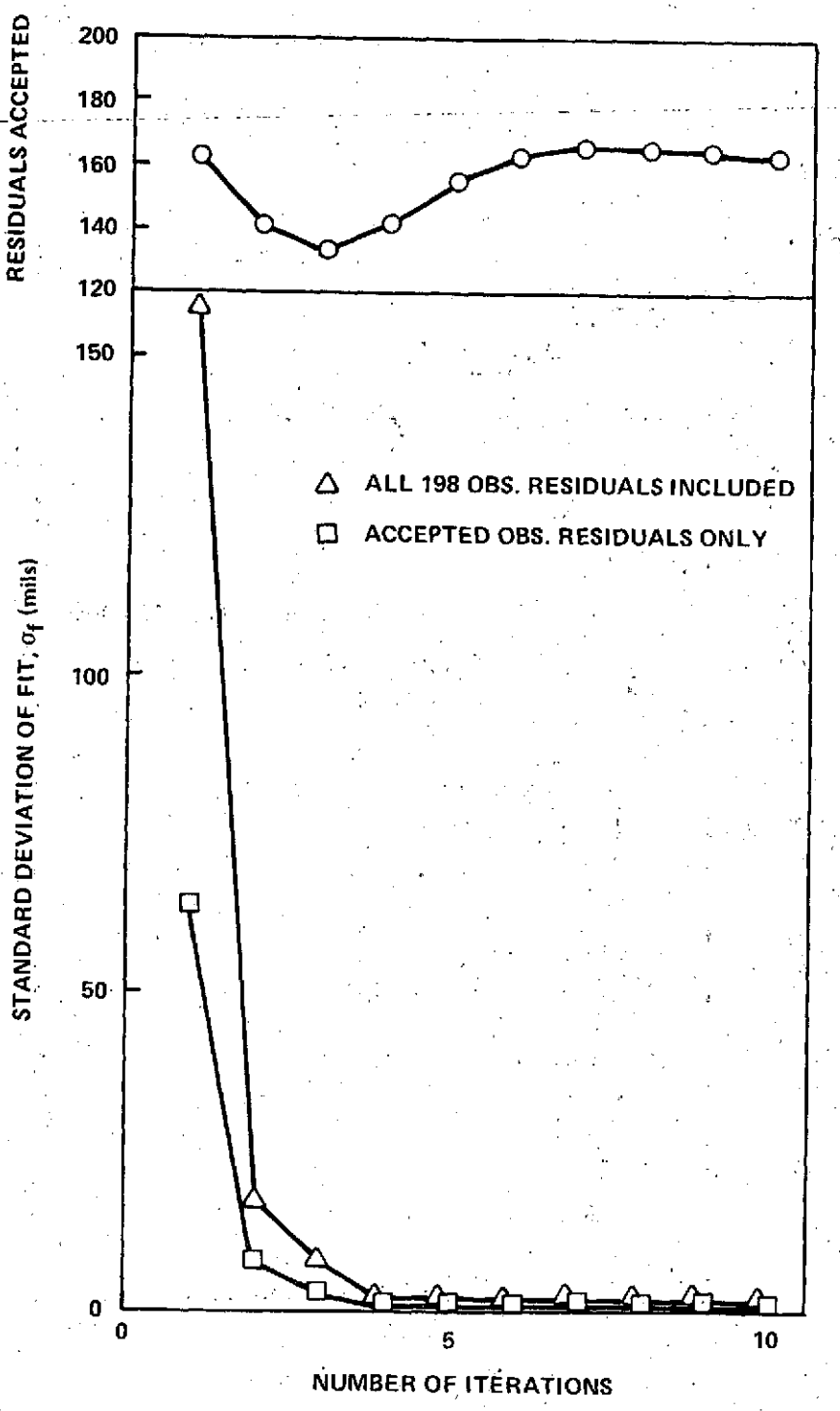

Figure 7. Standard Deviations of Fit and the Number of Observational Residuals Accepted at Each Iteration of the Fitting Process for the Combined Data Solution

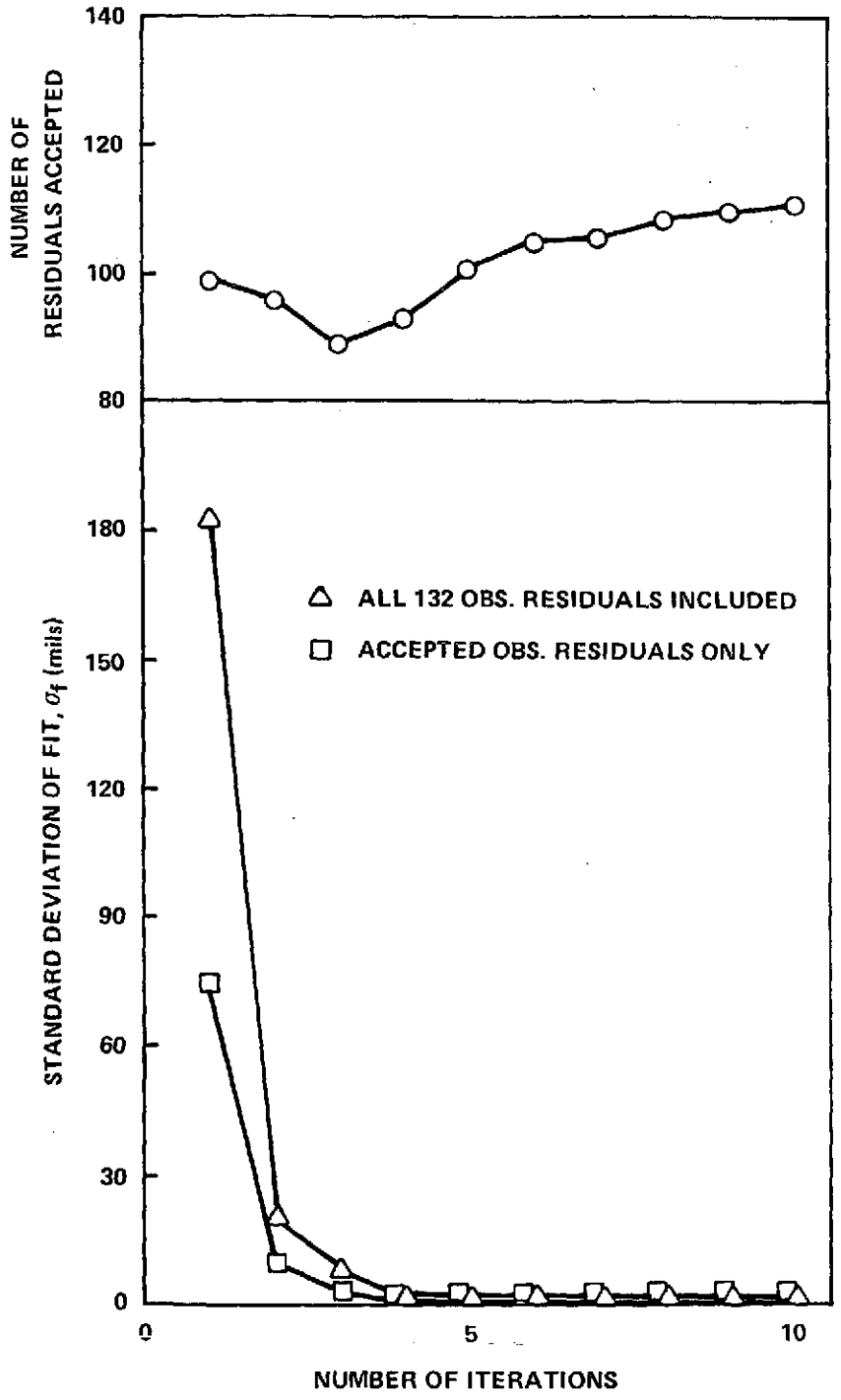

Figure 8. Standard Deviations of Fit and the Number of Observational Residuals Accepted at Each Iteration of the Fitting Process for the Quito Data Solution

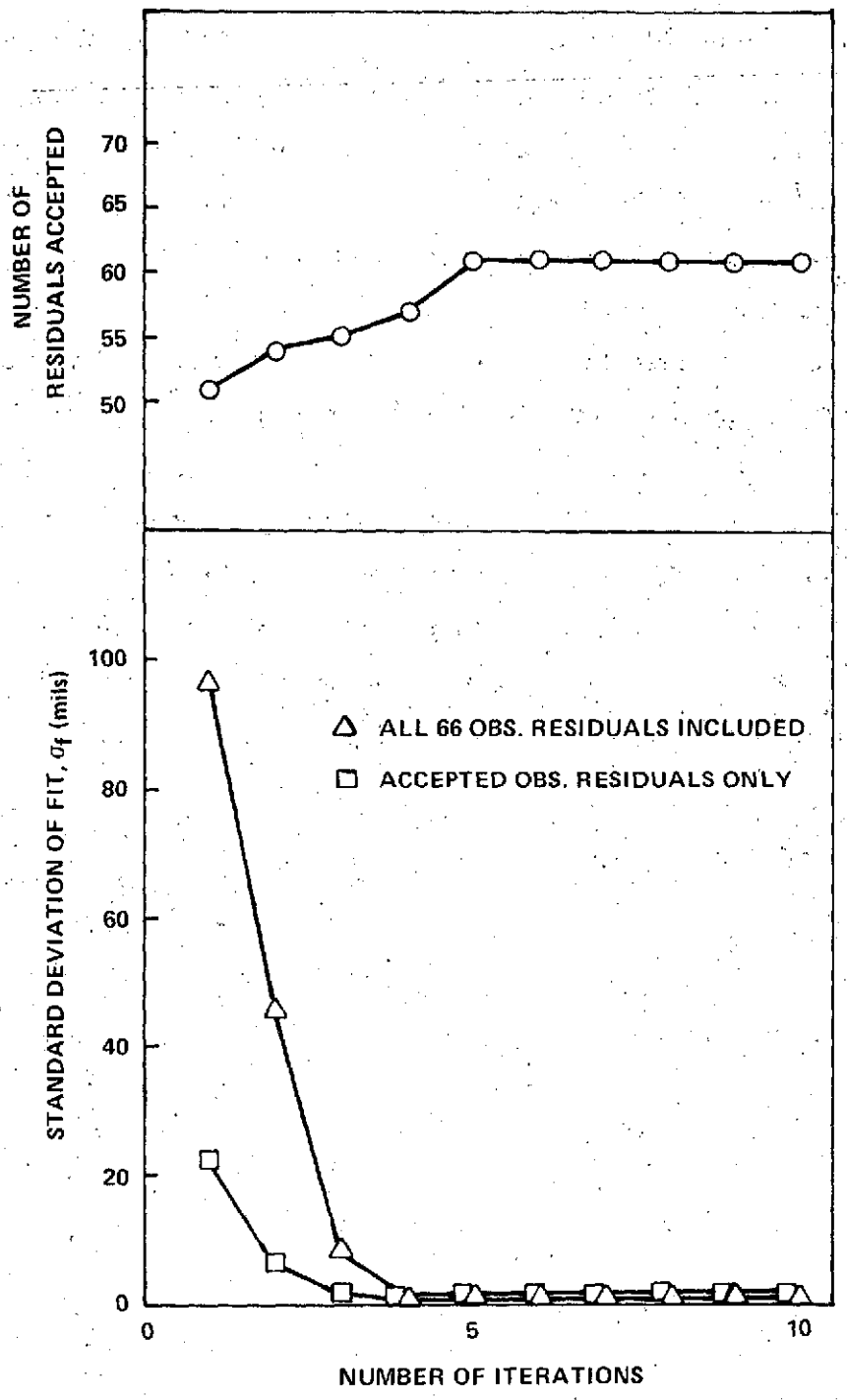

Figure 9. Standard Deviations of Fit and the Number of Observational Residuals Accepted at Each Iteration of the Fitting Process for the Kourou Data Solution

solution (reference case 2) and the Kourou data solution (reference case 3), which include totals of 132 and 66 observational residuals, respectively. The final values at convergence for the standard deviations of fit and for the number of observational residuals accepted for each of the three reference cases are given in Table 7. Note that the standard deviations converge in essentially monotonic fashion; this is not always so for the curve representing the number of accepted residuals.

This concludes the presentation of results for the three reference case investigations which were undertaken to provide a comparative basis for the post-flight differential correction analysis. In so doing, the subsidiary objectives of evaluating the CNES tracking data from Kourou, both in isolation and in combined solutions with NASA tracking data from Quito, have also been achieved. In order to accomplish the primary objectives of this investigation, a large number of further comparative case studies was conducted. The results of these comparative cases will be discussed in the following section.

PRESENTATION OF RESULTS FOR COMPARATIVE CASES

The primary objectives of this study, by way of paraphrase, are (1) to evaluate the Vinti spheroidal differential correction method as specifically applied to the near-equatorial and near-circular characteristics of the SAS orbit, and (2) to determine the capabilities of this differential correction method in a limited observational data environment, particularly with respect to data pairs, tracking station passes, and data block time duration. Reference cases 2 and 3 have already demonstrated that the capability exists for single tracking station solutions provided that sufficient observational data pairs and station passes are available over an appropriately long time duration. The independent and distinct comparative differential corrections of orbital elements performed to satisfy the primary objectives utilize the same sets of geophysical parameters and initial conditions, as tabulated in Tables 4 and 5, respectively.

Table 8 displays basic quantitative information for sixteen comparative cases, which are designated by continuing sequential integers for convenience. In fact, the sequence shown for these cases represents the actual order in which they were produced during the course of research leading to the current paper. The totality of comparative cases is subdivided into sets of two or three cases each according to the purpose and outcome of a particular line of investigation. Cases 4, 5, and 6 represent attempts at progressive reduction in the time span of the observational data from both tracking stations as compared to Case 1 in Table 6. In each succeeding case, the time span is approximately halved, while the number of observational pairs and the number of passes also decrease correspondingly. The proportion of Kourou passes increases as the reduction in the time span progresses, since the Kourou data available are heavily concentrated in the early orbit determination interval, as mentioned previously. Case 4 corresponds to observational data spanning 11 orbital revolutions of SAS-I, Case 5 corresponds to 5½ orbital revolutions, and

Table 8

Iterated Fittings of Observational Arcs by Differential Correction: Comparative Cases

Case Number	Observational Pairs	Time Span	Number of Passes	Stations Included*	Residual Acceptance Criterion*	Convergence Attained	Iterations Required**
4	57	$17^h\,09^m\,53^s$	19	11Q-8K	1σ	yes	8
5	33	$8^h\,31^m\,42^s$	11	6Q-5K	1σ	yes	7
6	18	$3^h\,32^m\,23^s$	6	3Q-3K	1σ	yes	8
7	12	$1^h\,50^m\,11^s$	4	2Q-2K	1σ	no	(2)
8	12	$1^h\,50^m\,11^s$	4	2Q-2K	2σ	yes	5
9	12	$1^h\,50^m\,11^s$	4	2Q-2K	3σ	yes	6
10	6	$7^m\,53^s$	2	1Q-1K	1σ	no	(1)
11	6	$7^m\,53^s$	2	1Q-1K	2σ	no	(1)
12	22	$7^m\,53^s$	2	1Q-1K	1σ	no	(1)
13	22	$7^m\,53^s$	2	1Q-1K	2σ	no	(1)
14	9	$1^h\,42^m\,47^s$	3	2Q-1K	1σ	no	(1)
15	9	$1^h\,42^m\,47^s$	3	2Q-1K	2σ	yes	6
16	6	$1^h\,42^m\,47^s$	2	Q	1σ	no	(1)
17	6	$1^h\,42^m\,47^s$	2	Q	2σ	no	(2)
18	6	$1^h\,42^m\,47^s$	3	2Q-1K	1σ	no	(2)
19	6	$1^h\,42^m\,47^s$	3	2Q-1K	2σ	yes	8

* See footnotes to Table 6.

**In the case of non-convergence of the iterated fitting process, the number indicated represents the iteration during which divergence occurred. This number is distinguished by being placed within parentheses.

Case 6 corresponds to 3 orbital revolutions. (In Case 5, the fractional revolution indicates that observational data from only one of two available station passes were included during the final revolution.) In all three cases, the extensive form of data coverage is again utilized, and the acceptance criterion for the observational residuals is set at one sigma. Such a one-sigma criterion produced convergence in all three comparative cases in approximately the same number of iterations as was required for the three reference cases (Table 6).

Cases 7, 8, and 9 represent attempts at further reduction in the time span of the observational data from both tracking stations. In these three cases, four passes and 12 observational data pairs in the extensive form of coverage for the first 2 orbital revolutions are utilized in the differential correction. This reduces the time span of the data to less than two hours. (Note that this "time span" refers to the length of the interval between the first and last observation included in the data block, and this time period consequently is not equivalent to that calculated from the product of the number of orbital revolutions and the length of the orbital period. Thus, although the data block spans two orbital revolutions, the time span as given is barely longer than a single orbital revolution.) In Case 7, the iterated fitting process was found to diverge after 2 iterations. During the first iteration, seven of the total of 24 direction cosine observations (12 pairs) failed to meet the one-sigma criterion, and during the second iteration, the number of failures rose to 11 observations. In order to decrease this high failure rate, Case 8 employed a two-sigma criterion with precisely the same observational data block under consideration. In Case 8, only two of the total of 24 direction cosine observations failed to meet the two-sigma criterion during the first iteration of the fitting process. Convergence was attained after 5 iterations, with only a single observation omitted in the final converged solution with the two-sigma criterion. As a final check, Case 9 was produced in which a three-sigma criterion was adopted, again with

precisely the same data block under consideration. In Case 9, none of the 24 observations failed to meet the three-sigma criterion during any of the six iterations required for convergence of the fitting process. These results are in general accordance with statistical theory for normal (Gaussian) distributions, which states that 95.45 percent of the observations will be included in the fitting process using a two-sigma criterion and 99.73 percent with a three-sigma criterion. These percentage values hold approximately for moderately skewed distributions (Reference 5).

Cases 10 and 11 attempt yet further reductions in the time span of the observational data from both tracking stations during the first orbital revolution only. One pass from each station is included, with a total of 6 observational pairs in the extensive data coverage form, and the time span is a mere 8 minutes. In Case 10, using a one-sigma criterion, five of the total of 12 observations were excluded during the first iteration of the fitting process and divergence resulted. In Case 11, a two-sigma criterion was employed, and, although none of the 12 observations in the same data block was omitted during the first iteration, divergence occurred again at the same point. Since convergence was not attained despite the fact that all 12 observations were included in the fitting process, there was little reason to attempt a differential correction utilizing a three-sigma criterion.

Instead, in Cases 12 and 13, the intensive data coverage form of 11 observational data pairs per pass is adopted for the same two passes during the first orbital revolution spanning less than 8 minutes. Neither case produces convergence. In Case 12, using a one-sigma criterion, 20 of the total of 44 direction cosine observations were excluded during the first and only iteration of the fitting process prior to divergence. Use of a two-sigma criterion in Case 13 produced acceptance of all 44 residuals in the first iteration, but still led to divergence after this first fitting. Thus, regardless of the residual acceptance criterion or the form of observational data coverage, a successful differential

correction did not result when the time span of the observations was reduced to only 8 minutes.

In Cases 14 and 15, a second Quito pass from the second orbital revolution is included to extend the observational time span to somewhat under 2 hours. Reversion to the extensive data coverage form of 3 observational data pairs per pass is, however, made. Thus, Cases 14 and 15 represent a slight reduction in the data time span from Cases 7, 8, and 9 considered previously, in which one Kourou pass instead of two is now included. The results in the current cases are, in fact, similar to the earlier results. In Case 14, using a one-sigma criterion, six of the total of 18 observations are excluded from the solution during the first iteration, and divergence immediately occurs. However, use of a two-sigma criterion in Case 15 produces convergence in which at most only one observational residual is rejected during any of the six iterations required. To this point of the investigation, Case 15 represents the minimum time span and the minimum number of observations and station passes for which a successful differential correction has been produced.

For Cases 16 and 17, the observational time span remains unchanged but the 3 observational pairs of data from the single Kourou pass are removed from consideration. Thus, the data block consists of 3 pairs of direction cosine data observed during each of the first two consecutive Quito passes only. This reduction to two passes, however, leads to non-convergence for both residual acceptance criteria utilized. In Case 16, using a one-sigma criterion, three of the total of 12 observations are rejected during the first and only iteration prior to divergence, while in Case 17, using a two-sigma criterion, all 12 observations are included in both iterations prior to divergence.

Finally, Cases 18 and 19 invoke a modified form of extensive data coverage wherein only two observational pairs of direction cosines are utilized from each of the first three station passes. The two observations selected from each pass are the first and last recorded direction cosines, i.e., the central

observational pair of the extensive data coverage form is omitted in these two cases. Thus, although the data block time span of Cases 18 and 19 is identical to that considered in Cases 14 through 17 and the number of observations included in Cases 18 and 19 is identical to that included in Cases 16 and 17, an additional pass is accommodated in Cases 18 and 19 as compared to Cases 16 and 17. Use of a one-sigma criterion in Case 18 results in the rejection of 4 and then 5 observations of the total of 12 observational residuals during the two iterations preceding divergence. However, the two-sigma criterion utilized in Case 19 produces convergence in which at most only one observational residual is rejected during any of the eight iterations required. This successful differential correction represents an improvement in minimizing the number of observations required in the solution over that of Case 15, although the time span of the observations and the number of passes required are the same in the two converged cases.

Further quantitative information relating to these sixteen comparative cases of differential correction is given in Table 9. The description provided previously of the parameters displayed in Table 7 applies equally well to Table 9. The values shown in the various columns of the table are those of the respective parameters at convergence, i. e., values at the iteration indicated in the final column of Table 8 for each case. For cases in which divergence occurred, the number of accepted residuals, and the percentage this number represents of the total number of conditional equations, are based upon results achieved at the final iteration prior to divergence. (In such cases, the final column of Table 8 provides the iteration number at which divergence actually occurred.) In cases of divergence, values for the standard deviations of fit and the converged orbital elements are, of course, not available. The proportions of accepted observational residuals are in general agreement with those of a normal distribution for the respective cases of a one-sigma, two-sigma, or three-sigma residual acceptance criterion, as shown in Table 8. In each case that a 2σ or 3σ

Table 9

Values at Convergence of Iterated Differential Correction: Comparative Cases

Case Number	Total Conditional Equations	Accepted Residuals	Percentage of Total	Standard Deviation of Fit (all)*	Standard Deviation of Fit (accepted)*	Converged Semi-Major Axis a (km)	Converged Eccentricity e	Converged Inclination i (deg)
4	114	92	80.7	0.696	0.373	6917.400	0.002881	3.0306
5	66	51	77.3	0.421	0.186	6917.341	0.002878	3.0333
6	36	31	86.1	0.676	0.231	6917.366	0.002799	3.0336
7	24	13	54.2	-	-	-	-	-
8	24	23	95.8	0.353	0.268	6917.376	0.002968	3.0427
9	24	24	100.	0.338	0.338	6917.350	0.002977	3.0429
10	12	7	58.3	-	-	-	-	-
11	12	12	100.	-	-	-	-	-
12	44	24	54.5	-	-	-	-	-
13	44	44	100.	-	-	-	-	-
14	18	12	66.7	-	-	-	-	-
15	18	17	94.4	0.434	0.266	6917.374	0.003020	3.0440
16	12	9	75.0	-	-	-	-	-
17	12	12	100.	-	-	-	-	-
18	12	7	58.3	-	-	-	-	-
19	12	12	100.	0.467	0.467	6917.339	0.002967	3.0435

*See footnote to Table 7.

criterion was invoked, at least 94 percent of the residuals were accepted. The acceptance levels for the one-sigma criterion cases varied somewhat about the prediction for a normal distribution. The values for all the converged elements displayed in Table 9 show very minor departures from the converged element values of Table 7 for the three reference cases. However, these minor departures are wholly negligible when contrasted with the improvements made to the corresponding initial values for the respective orbital elements given in Table 5. The results again demonstrate that each successful differential correction included in Tables 8 and 9 produces independently very nearly the same final converged values for the three orbital elements indicated. (The same conclusion holds for the remaining three orbital elements, which are omitted from the table for reasons of legibility.) The effectiveness of all differential corrections leading to convergence is further corroborated by the low values of the standard deviations of fit, as shown in Table 9.

Table 10 displays basic quantitative information for thirteen further comparative cases, similarly designated by continuing sequential integers for convenience and in the actual order produced during investigation. These comparative cases represent further attempts at minimization of the required number of observations, number of tracking station passes, and corresponding time span of the data block to achieve a converged differential correction solution. Cases 20 and 21 are additional endeavors to produce a successful differential correction with observational data from only two passes, beyond the failures of Cases 10 through 13 and 16 and 17, as shown in Table 8 and discussed previously. In Cases 20 and 21, the same data block time span is considered as in Cases 16 and 17, but the extensive form of data coverage of the latter cases is now expanded to the intensive form, with 11 observational data pairs per pass. The results, however, are no more promising in the current cases, since divergence occurs for both residual acceptance criteria utilized. In Case 20, using a one-sigma criterion, eleven of the total of 44 observational

Table 10

Iterated Fittings of Observational Arcs by Differential Correction: Further Comparative Cases

Case Number	Observational Pairs	Time Span	Number of Passes	Stations Included*	Residual Acceptance Criterion*	Convergence Attained	Iterations Required**
20	22	$1^h 42^m 47^s$	2	Q	1σ	no	(1)
21	22	$1^h 42^m 47^s$	2	Q	2σ	no	(2)
22	5	$1^h 42^m 32^s$	3	2Q-1K	1σ	no	(2)
23	5	$1^h 42^m 32^s$	3	2Q-1K	2σ	no	(3)
24	5	$3^h 24^m 33^s$	5	3Q-2K	1σ	yes	8
25	4	$1^h 49^m 41^s$	4	2Q-2K	1σ	no	(1)
26	4	$1^h 49^m 41^s$	4	2Q-2K	2σ	yes	7
27	3	$1^h 42^m 17^s$	3	2Q-1K	1σ	no	(0)
28	3	$1^h 42^m 17^s$	3	2Q-1K	2σ	yes	6
29	22	$1^h 50^m 11^s$	2	1Q-1K	1σ	no	(3)
30	22	$1^h 50^m 11^s$	2	1Q-1K	2σ	no	(2)
31	11	30^s	1	Q	1σ	no	(1)
32	11	30^s	1	Q	2σ	no	(1)

*See footnotes to Table 6.
**See footnote to Table 8.

residuals are rejected during the first and only iteration prior to divergence. (Note that this is exactly the same ratio of rejected residuals as in Case 16.) In Case 21, using a two-sigma criterion, all 44 observations are included in both iterations prior to divergence (similar to the situation of Case 17).

Cases 22 and 23 are attempts to reduce the successful three-pass differential corrections of Cases 15 and 19 to a smaller number of observations. The extensive data coverage form is further modified beyond that utilized in Cases 18 and 19 so that now two observational pairs (the first and last recorded) from each of the first two passes (one at Quito and one at Kourou) and only a single observational pair (the central pair) from the third pass (at Quito) are included. As contrasted with Cases 18 and 19, the current cases replace the first and last observational pair from the third pass with the central observational pair from that same Quito pass. Thus, the time span of the data block in Cases 22 and 23 is reduced slightly from that of Cases 18 and 19 by the amount of 15 seconds, which represents one-half the duration of a station pass. The omission of a single observational pair from the final pass results in divergence for both residual acceptance criteria used, as contrasted with the successful convergence of Case 19 previously. In Case 22, using a one-sigma criterion, four of the total of 10 observational residuals are rejected during each of the two iterations prior to divergence. Note that this results in the use of only six equations of condition during the fitting process to determine the six orbital elements, i.e., an exact solution, rather than a true least squares solution, may be found under these circumstances. In such a special case, the set of accepted conditional equations is identical to the reduced system of normal equations, and the solution may be obtained directly by use of the Gaussian elimination method (Reference 5). In Case 23, using a two-sigma criterion, all 10 observational residuals are included in all three iterations of the fitting process, a true least squares solution is possible at each iteration, but divergence occurs.

In Case 24, an attempt is made to determine whether a successful differential correction utilizing only five observational pairs is possible under any circumstances. In this instance, the time span of the data block is increased substantially to just about twice the value it had in the immediately preceding cases by including the central observational pair only from each of the first five passes. Thus, Case 24 corresponds to two full orbital revolutions of the SAS-I spacecraft plus observational data from the first of two available station passes during the third revolution. The use of a one-sigma residual acceptance criterion leads to convergence of the differential correction in 8 iterations, thus improving upon the results of Case 19 of Table 8 in terms of reducing the required number of observational pairs.

The concept of including only the single central observational pair of direction cosine data for each station pass is employed again in Cases 25 and 26. Here only the first four passes from the first two orbital revolutions are considered. This leads to a data block time span only some 30 seconds less than that of Cases 7 through 9 of Table 8, in which the same four passes were considered. (The difference of 30 seconds in time represents one-half the duration of a station pass at each of the first and last passes included, by virtue of the fact that only the central observational pair is present in the current data block.) In Case 25, using a one-sigma criterion, two of the total of 8 observational residuals are rejected during the first iteration of the fitting process. This leads to an exact, rather than a true least squares, solution with the remaining six equations of condition, as discussed previously. However, on the second iteration, four observational residuals fall outside the 1σ tolerance, leaving only four equations of condition with which to determine six orbital elements. A mathematically unique solution is not possible under such circumstances, and the differential correction may be said to diverge. In Case 26, using a two-sigma criterion, at most only one observational residual is rejected during the iterated fitting process, so that a true least squares solution

is possible at each iteration. In fact, the differential correction converges after 7 iterations in this case, thereby further improving the results of Case 24 with respect to reducing the required number of observations.

In Cases 27 and 28, the minimum form of data coverage using only the single central observational pair for each station pass is again utilized in an attempt to achieve the ultimate reduction in the number of observational pairs. The first three station passes are considered, with a resulting data block time span only some 30 seconds less than that of Cases 14, 15, 18, and 19 of Table 8 and some 15 seconds less than that of Cases 22 and 23. All differences in the time spans specified are due to the slight changes in data coverage for the same three passes. Since only three observational pairs of direction cosines are included in the data block, even a single rejection of an observational residual at any iteration during the fitting process will cause the differential correction to diverge due to the lack of uniqueness of the solution. Even with the acceptance of all observational residuals at each iteration of the fitting process, a true least squares solution is not possible, although an exact solution may result. In Case 27, using a one-sigma criterion, two of the total of 6 observational residuals fall outside the specified tolerances even prior to the first iteration of the fitting process, thereby resulting in divergence. This explains the reason that a zero is recorded in the final column of Table 10 for this case. However, in Case 28, using a two-sigma criterion, all observational residuals are accepted at each iteration of the fitting process, and convergence of the differential correction to an essentially zero value of the standard deviation of fit occurs within 6 iterations. This successful differential correction using only three observational pairs represents, of course, the ultimate minimum possible in theory.

Several further attempts were made to produce a converged differential correction using observational data from fewer than three passes, however. Recall that Cases 10 through 13 (refer to Table 8) were unsuccessful in producing

convergence using observations from the first two passes of the first orbital revolution. Likewise, Cases 16 and 17 and also Cases 20 and 21 were similarly not successful in producing convergence using data from the first two Quito passes of the first two revolutions. Cases 29 and 30 utilize observational data in the intensive coverage form (11 observational pairs for each pass) from the first Quito pass during the first revolution and from the second Kourou pass during the second revolution. Thus, the data block time span is slightly longer but comparable to that of Cases 16-17 and Cases 20-21. In Case 29, using a one-sigma residual acceptance criterion, first 12, then 21, and finally 19 of the total of 44 observations are rejected during the three iterations preceding divergence. In Case 30, using a two-sigma criterion, all 44 observational residuals are accepted in both iterations prior to divergence, but the end result is similar.

Finally, in Cases 31 and 32, the intensive data coverage form is utilized for the single first Quito pass only. The data block time span here is a mere 30 seconds. These cases were admittedly unlikely to produce convergence of the differential correction, but they were attempted in the interests of investigative thoroughness. Both cases quickly lead to divergence after a single iteration, despite the fact that the two-sigma criterion of Case 32 leads to acceptance of all 22 observational residuals.

Additional quantitative information relating to these thirteen further comparative cases of differential correction appears in Table 11. The values of the various parameters in the table are those that occur either at convergence or just prior to divergence, as applicable and as indicated by the iteration number included in the final column of Table 10 for each case. Note that utilization of a two-sigma acceptance criterion results in the acceptance of the totality of observational residuals in all applicable cases, except one case in which only a single residual is rejected from the converged solution. The standard deviation of fit including all observational residuals for the converged

Table 11

Values at Convergence of Iterated Differential Correction: Further Comparative Cases

Case Number	Total Conditional Equations	Accepted Residuals	Percentage of Total	Standard Deviation of Fit (all)*	Standard Deviation of Fit (accepted)*	Converged Semi-Major Axis a (km)	Converged Eccentricity e	Converged Inclination i (deg)
20	44	33	75.0	--	--	--	--	--
21	44	44	100.	--	--	--	--	--
22	10	6	60.0	--	--	--	--	--
23	10	10	100.	--	--	--	--	--
24	10	8	80.0	2.974	0.183	6917.354	0.003036	3.0096
25	8	4	50.0	--	--	--	--	--
26	8	7	87.5	0.430	0.068	6917.363	0.003003	3.0397
27	6	4	66.7	--	--	--	--	--
28	6	6	100.	0.000	0.000	6917.354	0.003181	3.0447
29	44	25	56.8	--	--	--	--	--
30	44	44	100.	--	--	--	--	--
31	22	9	40.9	--	--	--	--	--
32	22	22	100.	--	--	--	--	--

*See footnote to Table 7.

solution of Case 24 is comparatively large, but when the two rejected residuals for this converged solution are excluded, the standard deviation of fit assumes a value more compatible with previous results. Both standard deviations of fit for the converged solution of Case 28 are shown as zero values inasmuch as such a solution for a total of six conditional equations is necessarily exact. In fact, both standard deviations of fit were calculated to be non-zero values, although both considerably less than 10^{-6}, due to numerical truncation and round-off errors. Once again, the values for all the converged elements displayed in Table 11 show only minor departures from the converged element values of Table 7 for the three reference cases. In comparison with the minor departures previously noted in Table 9, only the converged inclination of Case 24 and the converged eccentricity of Case 28 noticeably depart from the respective converged values of the three reference cases. Such departures are, of course, due to the limited observational data blocks utilized in the converged differential corrections of Table 11. Even so, it is seen that the departures from the converged values of the reference cases are fairly insignificant when contrasted with the improvements made to the corresponding initial values for the respective orbital elements (refer to Table 5). As an example, the converged inclination of Case 24 represents an improvement Δi of 0.096 degree from the initial value for the inclination as shown in Table 5, while the converged inclination of Reference case 1 represents an improvement Δi of 0.118 degree from the initial value. Therefore, it may be concluded that each successful differential correction included in Tables 10 and 11 produces independently nearly equivalent final converged values for the orbital elements.

SUMMARY AND CONCLUSIONS

The efficacy of the differential correction process based upon the Vinti spheroidal theory has been evaluated in the preceding analysis, insofar as the method applies to the near-equatorial and near-circular orbital characteristics of the SAS-I spacecraft. A total of 32 distinct differential corrections based upon the Vinti spheroidal theory has been presented and analyzed, and in no case were the nearly singular values of the orbital elements clearly responsible for difficulties in achieving convergence of the analytic solution. Of the total of 19 differential corrections attempted which failed to achieve convergence, it may be noted that five of these attempts subsequently resulted in converged solutions upon proper adjustment of the observational residual acceptance criterion. That is, the simple expedient of increasing the residual acceptance criterion from one sigma to two sigmas, and thereby increasing the proportion of observational residuals retained in the iterated fittings, produced a converged solution after the failures of Cases 7, 14, 18, 25, and 27, all of which were based upon a one-sigma criterion. Of the remaining 14 cases of differential correction divergence, it is seen that 12 of these cases occurred under the extremely demanding circumstance of attempting to provide a solution in the very limited data environment of two or fewer station passes. That is, Cases 10-11, 12-13, 16-17, 20-21, and 29-30 include observational data from two station passes only, while Cases 31-32 include data from but a single pass. It was not possible, during this study, to promote a converged differential correction solution based upon observational data from only two station passes. The remaining pair of non-converged differential corrections, viz., Cases 22-23, utilized observational data from three station passes during the first two orbital revolutions. In three other cases utilizing observations from the same three station passes and with a two-sigma residual acceptance criterion (viz., Cases 15, 19, and 28), convergence of the differential correction process did, in fact, result. The

converged Cases 15 and 19 required nine and six pairs, respectively, of observational data from these three station passes, as opposed to merely five pairs of observational data included in the attempts of Cases 22-23. However, Case 28 required only the theoretical minimum of three pairs of observational data from the first three station passes to achieve convergence. Thus, the divergence of Case 23, in particular, must be considered an anomaly, inasmuch as the omission of two of the five pairs of observational data results in convergence for the same three station passes in Case 28. In sum, with the possible exception of this single anomalous case, given a minimum observational data block consisting of three station passes and a properly adjusted residual acceptance criterion, the Vinti spheroidal differential correction method produced successful convergence under a wide variety of trials and circumstances for a near-equatorial and near-circular satellite orbit as typified by the SAS-I trajectory.

The capabilities of the differential correction procedure in a limited observational data environment have also been ascertained during the course of this study. It was readily determined that observational data acquired at a single tracking station are easily sufficient to provide an accurate converged solution for the definitive orbit. This determination resulted from the so-called reference case differential corrections. Also, as stated above, a minimum observational data block consisting of three station passes was required to achieve convergence of the orbital solution during this investigation. In addition, it was found that three observational pairs of direction cosine data, the minimum number possible for a uniquely determined solution in theory, are sufficient to promote convergence, if properly selected and distributed over the time span of at least three station passes. Finally, the minimum time duration of the observational data block required to achieve convergence was found to be one orbital revolution plus a portion of a second revolution containing the first of two station passes only. Specifically, this time span

was approximately 102 minutes for the current study. However, it is to be noted that this time span is highly dependent upon the relative geographical locations of the tracking stations providing observational data. The use, in this analysis, of only two tracking stations, which are located within 26 degrees in longitude of one another, created a rather unusually difficult situation for orbit determination, as compared to the more typical case of non-equatorial orbits of medium or high inclination. Thus, it is believed that with tracking stations more evenly distributed in longitudinal location, than as is the case for the current study, the minimum time span required to achieve convergence of the differential correction might be substantially reduced.

Finally, this post-flight differential correction analysis has subjected the CNES tracking data from the Kourou station to rigorous quality testing. These data have been utilized in numerous differential correction solutions, both independently and also in conjunction with additional NASA Minitrack data. The three reference case differential corrections of orbital elements by iterated fittings of observational arcs clearly demonstrate that the Kourou tracking data are wholly valid and internally consistent, as well as being fully compatible with NASA tracking data. The independent differential corrections using tracking data from Kourou only and from Quito only produce essentially the same set of final converged values for orbital elements as one another and as the combined data solution using interspersed observations from both stations. Hence, there is, in practice, no need to distinguish between the sources of the two types of direction cosine observational data.

ACKNOWLEDGMENTS

The author wishes to express appreciation to J. S. Watson for substantial contributions in producing the numerical results presented herein by digital computer calculations. Acknowledgments are also due to L. H. Anderson for several helpful discussions and suggestions during the course of the analysis, to E. R. Watkins, Jr. and D. J. Cannaday for assistance in providing the spacecraft observational data utilized, and finally to A. J. Fuchs for useful criticism suggested during review of the manuscript.

REFERENCES

1. Walden, Harvey and Watson, Stan, "Differential Corrections Applied to Vinti's Accurate Reference Satellite Orbit with Inclusion of the Third Zonal Harmonic," NASA Technical Note D-4088, August 1967.

2. Vinti, John P., "Invariant Properties of the Spheroidal Potential of an Oblate Planet," Journal of Research of the National Bureau of Standards (U. S.), Volume 70B (Mathematics and Mathematical Physics), Number 1, pages 1-16, January-March 1966.

3. Vinti, John P., "Inclusion of the Third Zonal Harmonic in an Accurate Reference Orbit of an Artificial Satellite," Journal of Research of the National Bureau of Standards (U. S.), Volume 70B (Mathematics and Mathematical Physics), Number 1, pages 17-46, January-March 1966.

4. Vinti, John P., "Improvement of the Spheroidal Method for Artificial Satellites," The Astronomical Journal, Volume 74, Number 1, pages 25-34, February 1969.

5. Walden, Harvey, "Orbital Prediction and Differential Correction Using Vinti's Spheroidal Theory for Artificial Satellites," NASA Technical Note D-3803, March 1967.

6. Bonavito, N. L., Watson, Stan, and Walden, Harvey, "An Accuracy and Speed Comparison of the Vinti and Brouwer Orbit Prediction Methods," NASA Technical Note D-5203, May 1969.

7. "Project Development Plan: Small Astronomy Satellite (SAS)," Marjorie R. Townsend, Project Manager, Goddard Space Flight Center, April 1968.

8. "NASA-GSFC Operations Plan 6-70, Small Astronomy Satellite (SAS-A)," Document No. X-513-70-417, Project Operations Support Division, Goddard Space Flight Center, November 1970.

9. Walden, Harvey, "Early Orbital Computation Procedures for the Small Astronomy Satellite (SAS-A) Mission," Internal Memorandum No. 552-233, Goddard Space Flight Center, November 27, 1970.

10. "Scout Vehicle S-175C, SAS-A Payload Mission, Pre-Flight Trajectory Data," Design Information Release 23-DIR-1108, Rev. B, LTV Aerospace Corporation, Missiles and Space Division, November 30, 1970.

11. Walden, Harvey, "Early Orbital Determination for the Small Astronomy Satellite (SAS-A)," Director's Weekly Report, Goddard Space Flight Center, December 18, 1970.